Path Planning and Localization for Mobile Anchor Based Wireless Sensor Networks

Ecenaz Erdemir, T. Engin Tuncer

Electrical and Electronics Engineering Department, METU, Ankara, Turkey

{ecenaz , etuncer}@metu.edu.tr

Abstract—In wireless sensor networks, anchor positions play an important role for accurate localization. For mobile anchor (MA) based scenarios, both the efficiency of the path planning algorithm and the accuracy of the localization mechanism are critical for the best performance. In this work, an adaptive path planning algorithm is proposed based on Gauss-Markov mobility model, while the sensors are localized using alternating minimization approach. Path planning, which combines the velocity adjustment, the perpendicular bisector and the virtual repulsive strategies, is improved by developing virtual attractive force strategy. The surveillance area is divided into grids and a virtual attractive force is applied to the MA in sparsely and densely populated areas. For localization, the non-convex optimization problem is converted into a bi-convex form and solved by alternating minimization algorithm leading to a shorter MA path. The simulation results show that introducing the virtual attractive strategy increases the path planning accuracy and cover more surveillance region using less energy. Furthermore, compared to the linear localization method, the localization accuracy increases when the alternating minimization is used.

Index Terms—Dynamic path planning, mobility model, mobile-anchor, sensor network localization, alternating minimization.

I. INTRODUCTION

Wireless sensor networks (WSNs) have been used in military surveillance, fire detection, target tracking and wireless security [1]. Sensor localization problem contains large number of unknown sensors randomly distributed in a region [2], [3]. WSN scenarios can be classified as range-free and range-based schemes. While range-free algorithms use connectivity between sensors and anchors, range-based algorithms use node-to-node distances or angles to localize sensors [4]. In this work, range-based scenario is investigated and TOA measurements are used for localization. In a WSN, anchor node positions play an important role for improving the localization accuracy. However, increasing the number of costly anchors also increases the cost of the localization process. Moreover, in static anchor scenarios, all anchor nodes become useless after the localization process. Hence, using a mobile anchor with the ability to broadcast its position decreases the cost of the localization [5]. In this work, a path planning algorithm based on Gauss-Markov (GM) mobility is proposed. In addition to the velocity adjustment, the perpendicular bisector and the virtual repulsive force strategies in [5], a virtual attractive force is defined in this paper to control the velocity and the direction of the mobile anchor. Besides, a sensor can be localized in 2-D, if there are at least three neighboring anchors in its communication range [6]. When there is no guarantee for three or more neighboring anchors, localization problem can

be solved by the proposed optimization algorithm effectively. In this work, limitations of the path planning algorithm in [5] are eliminated by proposing a virtual attractive force strategy and a novel optimization method for the localization.

II. SYSTEM MODEL

Consider N stationary sensors which are randomly distributed over an $L \times L$ surveillance area and a mobile anchor (MA) carrying a GPS receiver. The node positions created by the MA are represented by the vectors $\{\mathbf{a}_1, ..., \mathbf{a}_M\}, \mathbf{a}_n \in R^2$, and the sensor positions by the vectors $\{\mathbf{x}_1, ..., \mathbf{x}_N\}, \mathbf{x}_i \in R^2$. While (x_i, y_i) components of sensor coordinates $\mathbf{x}_i$ are unknown, the mobile anchor receives its position with GPS at each move. All sensors and the MA have communication ranges with the same radius R. The main problem is to estimate unknown sensor positions using node-to-node distances between sensors and the anchor. In this scenario, the MA follows a path and creates anchor nodes in time. When it enters the communication range of a sensor, the MA sends its position information to the sensor and receives an acknowledgment immediately. After enough anchor information is sent to the sensor, it is localized and the coordinates are transmitted with the acknowledgment packet. In part III and IV, the path planning algorithm and the localization mechanism for sensor coordinate estimation are explained respectively.

III. PATH PLANNING ALGORITHM

In this work, an adaptive path planning algorithm based on the GM mobility model is proposed. As in [5], the model can be described by

$$p_n = \alpha p_{n-1} + (1 - \alpha)\bar{p} + \sqrt{1 - \alpha^2} p_{x_{n-1}} \qquad (1)$$

$$d_n = \alpha d_{n-1} + (1 - \alpha)\bar{d} + \sqrt{1 - \alpha^2} d_{x_{n-1}} \qquad (2)$$

where p_n and d_n are the velocity and the direction of the MA at time n; α , where $0 \leq \alpha \leq 1$, is the parameter which is used to vary randomness; $\bar{p}$ and $\bar{d}$ are constant mean values of the velocity and the direction as $n \to \infty$; $p_{x_{n-1}}$ and $d_{x_{n-1}}$ are independent, zero mean Gaussian random variables. The next position of the MA is decided by the current location, velocity and direction. The position of the mobile anchor at time n is described by

$$x_n = x_{n-1} + p_{n-1} cos(d_{n-1}) \qquad (3)$$

$$y_n = y_{n-1} + p_{n-1} sin(d_{n-1}) \qquad (4)$$

where x_n and y_n are the MA coordinates at time n; d_{n-1} is the direction of the MA at time $n - 1$.

In the proposed path planning algorithm, the velocity adjustment, the perpendicular bisector, the virtual repulsive force

and the virtual attractive force strategies are used to control the velocity and direction of the mobile anchor.

A. Velocity Adjustment Strategy

(1) can be expressed in terms of the initial velocity p_0 as

$$p_n = \alpha^n p_0 + (1-\alpha^n)\bar{p} + \sqrt{1-\alpha^2}\sum_{i=0}^{n-1}\alpha^{n-i-1}p_{x_{n-1}} \quad (5)$$

According to (5), α^n becomes very small in time. Hence, p_n and d_n are found in the neighboring range of $\bar{p}$ and $\bar{d}$ [5]. Instead of moving with the mean pace, the MA velocity is adjusted according to the acknowledgments received from the sensors. Two cases are explained in the following sections for the velocity adjustment.

1) In the Communication Range:
Receiving an acknowledgment from a sensor, the MA decreases its velocity to stay in the communication range. Then it creates enough anchor positions for locating the sensor. Mean velocity $\bar{p}$ in (1) is set to $\bar{P}_{min}$ which is the minimum mean value of the MA pace. Then arranging (1), expression (6) is obtained as in [5],

$$p_n = p_{n-1} + (1-\alpha)(\bar{P}_{min} - p_{n-1}) + \sqrt{1-\alpha^2}p_{x_{n-1}} \quad (6)$$

As in (6), the MA velocity decreases when $\bar{P}_{min} = 0$ at time n.

2) Outside the Communication Range:
Receiving no acknowledgments, the MA increases its velocity to cover more surveillance region. Similar to (6), $\bar{p}$ is set to $\bar{P}_{max}$ and (1) is modified. The resulting expression (7) is obtained as in [5],

$$p_n = p_{n-1} + (1-\alpha)(\bar{P}_{max} - p_{n-1}) + \sqrt{1-\alpha^2}p_{x_{n-1}} \quad (7)$$

B. Perpendicular Bisector Strategy

When the MA enters the communication range of a sensor, it moves within the range until a predefined ξ number of non-collinear anchor is created. When the sensor is localized, the MA leaves the range.

In Figure 1, the bisector strategy is shown. The black circle is the sensor with the communication range R and the black triangles are the MA positions in time. Blue triangles are the possible MA coordinates at $n+1$. Solid lines are the paths followed by the MA until current time n; the blue line is the perpendicular bisector line between two consecutive anchor positions and the dashed line is the future path.
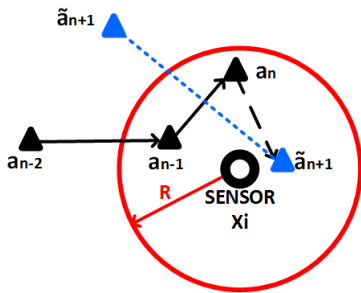

Fig. 1: The perpendicular bisector strategy.

In Figure 1, at n and $n-1$, two consecutive acknowledgments are received from the same sensor. The next MA

position is determined by the perpendicular bisector line shown by dots. $\tilde{\mathbf{a}}_{n+1}$ positions are two symmetric solutions for bisection and calculated by,

$$\tilde{\mathbf{a}}_{n+1} = \begin{bmatrix} \tilde{a}_{n+1,x} \\ \tilde{a}_{n+1,y} \end{bmatrix} = \begin{bmatrix} \frac{a_{n,x}+a_{n-1,x}}{2} \pm \sqrt{4\frac{d_{n+1,n}}{d_{n,n-1}}-1}(\frac{a_{n,y}-a_{n-1,y}}{2}) \\ \frac{a_{n,y}+a_{n-1,y}}{2} \pm \sqrt{4\frac{d_{n+1,n}}{d_{n,n-1}}-1}(\frac{a_{n-1,x}-a_{n,x}}{2}) \end{bmatrix} \quad (8)$$

where $\tilde{\mathbf{a}}_{n+1}$ is the solution for the possible MA position at $n+1$; $\tilde{a}_{n+1,x}$ and $\tilde{a}_{n+1,y}$ are x and y components of the vector $\tilde{\mathbf{a}}_{n+1}$; $a_{n,x}$ and $a_{n,y}$ are the components of the MA coordinate at time n; $d_{n+1,n}$ is the distance between $n+1^{st}$ and n^{th} anchor positions. As in (8), $\tilde{a}_{n+1,x}$ and $\tilde{a}_{n+1,y}$ coordinates have two symmetric solutions with respect to the line through $\mathbf{a}_n$ and $\mathbf{a}_{n-1}$. If the next MA position is chosen to be one of the $\tilde{\mathbf{a}}_{n+1}$ solutions and no acknowledgment is received, the MA moves to the symmetric position at time $n+2$.

If the MA leaves the range at n, the bisector is again applied to find $n+1$ position using the previous acknowledgment. When the MA is in the range of more than one sensor, a similar process is followed. For all cases, the perpendicular bisector strategy is repeated until the predefined ξ number of anchor positions are traversed.

C. Virtual Repulsive Force Strategy

In [5], the relation between the virtual repulsive force and the velocity is expressed by

$$\mathbf{F}_{RP} = m\frac{\mathbf{p}}{\Delta t} \quad (9)$$

where $\mathbf{F}_{RP}$ is the virtual repulsive force; $m(kg)$ is the anchor mass; $\mathbf{p}$ denotes the velocity vector of the MA and Δt is the sampling time interval. The virtual repulsive strategy is examined for two cases.

1) Outside the Surveillance Area:
After the MA leaves the surveillance region, a virtual repulsive force is applied to the anchor from the outside of the surveillance area. Hence, the MA returns to the region with the same velocity that it leaves the region at time $n-1$. The returning velocity and direction of the MA is denoted by

$$p_{returning} = p_{n-1}, \qquad d_n = D_{RP} \quad (10)$$

where $p_{returning}$ is the returning velocity; d_n is the direction vector in time n and D_{RP} is the direction determined by the virtual repulsive force of the outside region [5].

2) Inside the Surveillance Area:
Virtual repulsive force is defined as follows

$$\mathbf{F} = \begin{cases} 0, & u_{MA,i} > R \\ \mathbf{F}_{RP}, & u_{MA,i} < R \end{cases} \quad (11)$$

where $\mathbf{F}$ is the virtual force; $u_{MA,i}$ is the distance between the MA and i^{th} sensor [5]. If the MA enters the range of a localized sensor, the mobile anchor is repelled with a virtual repulsive force by the sensor. The choice for F_{RP} value is discussed in the simulations.

D. Virtual Attractive Force Strategy

In [5], Zhong et al. combines the velocity adjustment, the perpendicular bisector and the virtual repulsive force strategies with the GM mobility model. In this work, a virtual attractive force strategy is introduced. The proposed method is divided into two stages as follows.

1) Sparsely Populated Region:

In [5], when no acknowledgment is received in a sparsely populated area, the MA velocity is increased. However, there is no control over the direction. As stated in (2), the MA direction is a random variable according to the GM mobility model. This results inefficient path generation over the direction vector in the areas with low sensor density. Since there is no mechanism in [5] for preventing the MA staying in the same region, there is an accumulation of useless anchor positions. In this paper, the virtual attractive force strategy is proposed to improve the path generation efficiency and localization.

In Figure 2, a path planning example is given. In the proposed strategy, the surveillance region is divided into grids of $2R \times 2R$ as in Figure 2. The divided surveillance region is represented by a matrix $\mathbf{H}$ whose indexes are on the left and top positions of the grid structure. The matrix elements are the number of anchor positions in the corresponding grid and they are changed in time. If the current index exceeds a predefined threshold value λ, a virtual attractive force is applied to the mobile anchor. The grid applying the attractive force is chosen randomly among the closest minimum indexed grids.
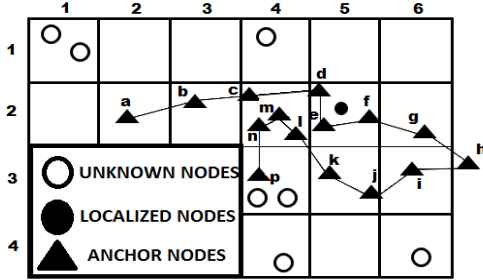

Fig. 2: Path planning algorithm.

In Figure 2, the MA moves starting from point **a**. After the first acknowledgment at **d**, the MA slows down moving to **e**. Then, anchor position **f** is generated using bisection. After the sensor is localized, the MA is repelled to **g** by the virtual repulsive force. Leaving the region at **h**, the MA is again repelled to **i** and continues to move randomly. When no acknowledgment is received at the current MA position, the corresponding index of $\mathbf{H}$ is checked. If the current index exceeds λ, a virtual attractive force is applied to the MA by the closest minimum indexed grids. For the Figure 2, $\mathbf{H}$ is given in (12) and $\lambda = 4$. The MA generates 4 anchor positions in the grid which corresponds to $\mathbf{H}_{2,4}$. Hence, virtual attractive force is applied to the MA by the closest minimum valued grid of $\mathbf{H}$ corresponding to $\mathbf{H}_{1,4}$ and $\mathbf{H}_{3,4}$. Then the MA moves to **p**.

$$\mathbf{H} = \begin{pmatrix} 0 & 0 & 0 & 0 & 0 & 0 \\ 0 & 1 & 1 & 4 & 3 & 1 \\ 0 & 0 & 0 & 1 & 2 & 1 \\ 0 & 0 & 0 & 0 & 0 & 0 \end{pmatrix} \qquad (12)$$

The virtual attractive force and the MA direction are defined by,

$$\mathbf{F} = \begin{cases} 0, & MA_{n(H_{i,j}<\lambda)} \\ \mathbf{F}_{AT}, & MA_{n(H_{i,j}\geq\lambda)} \end{cases}, \; d_n = D_{AT} \qquad (13)$$

where $\mathbf{F}_{AT}$ is the virtual attractive force applied; $MA_{n(H_{i,j}<\lambda)}$ is the case which the MA is in a grid with an index below λ at time n; $MA_{n(H_{i,j}\geq\lambda)}$ is the case which the MA is in a grid with an element exceeding the threshold value at time n. d_n is the direction vector at time n and D_{AT} is the direction to the closest minimum valued grid of $\mathbf{H}$.

2) Densely Populated Region:

When the MA enters the communication range of localized sensors, virtual repulsive force is applied to the MA by these sensors. However, if the MA is surrounded by localized sensors, it cannot cross them due to their virtual repulsive forces [5]. Zhong et al. proposes to remove the virtual repulsive force once, when the MA enters the range of a located sensor more than a predefined number of times, τ. On the other hand, this does not guarantee the MA to cross the localized sensors, since the direction vector is random. In this work, a better solution is proposed. When the MA enters the communication range of a localized sensor at least τ times, a virtual attractive force is applied to the MA. Similar to the sparse case, the direction of the virtual force is towards the closest minimum valued grid of $\mathbf{H}$.

The proposed path planning algorithm finds the solution for the direction control in sparsely and densely populated areas as described above. In the following part, the proposed localization mechanism is explained.

IV. LOCALIZATION METHOD

In this work, the localization algorithm is based on node-to-node distances obtained by TOA technique. In 2-D, sensor coordinates with at least three neighboring anchors are found by solving a linear set of equations [6]. On the other hand, in case there exists only two neighboring anchors, linear set of equations do not provide a solution. Decreasing the known positions in the sensor range creates position ambiguity. This ambiguity has symmetry and the sensor position can be one of the two symmetric positions.

The aim in using optimization is to localize sensors with few anchors. Considering the entire problem, localization with less anchors leads to smaller anchor threshold ξ for the path planning strategy. Besides, with smaller ξ, the MA stays less in the surveillance region to localize all sensors. This improvement decreases the process cost. Moreover, compared to solving linear set of equations, the localization accuracy is improved by the proposed optimization algorithm.

For the problem formulation, the Euclidean distance between n^{th} anchor and the ith sensor is denoted by

$$r_{ni} = \sqrt{(a_{n,x} - x_i)^2 + (a_{n,y} - y_i)^2} \qquad (14)$$

where $a_{n,x}$ and $a_{n,y}$ are the components of vector $\mathbf{a}_n$ representing the anchor coordinates.

The purpose of localization is to find the positions satisfying the distance constraints by minimizing the error function. This problem can be expressed by (15a-15c). e_{ni} in (15b) is called the error between the real distance r_{ni} and the estimated distance $\|\mathbf{a}_n - \mathbf{x}_i\|$ [3].

$$\underset{\mathbf{x}_i, e_{ni}}{\text{Minimize}} \quad \sum_{(n) \in \xi} e_{ni} \tag{15a}$$

$$\text{subject to} \quad e_{ni} = \|\mathbf{a}_n - \mathbf{x}_i\|_2^2 - r_{ni}^2 \tag{15b}$$

$$\mathbf{x_i}, \mathbf{a_n} \geq \mathbf{0} \tag{15c}$$

However, (15b) is non-convex due to equality. In this work, the non-convex problem formulation is modified to a biconvex form using alternating minimization algorithm (AMA) in [8]. This process does not guarantee the global optimum solution. However, the performance of AMA is significantly better than the alternative solution expressed in the simulation results.

V. ALTERNATING MINIMIZATION

The problem in (15) is not convex. One solution is converting the equality constraint to an inequality, i.e (16).

$$\|\mathbf{a}_n - \boldsymbol{x}_i\|_2 \leq r_{ni} \tag{16}$$

However, without a lower bound, (16) does not serve for the purpose. One way of avoiding the trivial solution is to have a cost function which includes a related term that is to be maximized as in (17).

$$\underset{\boldsymbol{x}_i}{\text{Maximize}} \quad \sum_{(n) \in \xi} \|\boldsymbol{a}_n - \boldsymbol{x}_i\|_2^2 \tag{17}$$

Besides, the quadratic cost function in (17), $\|\boldsymbol{a}_n - \boldsymbol{x}_i\|_2^2 = (\boldsymbol{a}_n - \boldsymbol{x}_i)^T (\boldsymbol{a}_n - \boldsymbol{x}_i)$, is converted into an affine form to bring the original problem into a convex structure. Thus, the cost function is modified as (18),

$$\|\boldsymbol{a}_n - \boldsymbol{x}_i\|_2^2 = (\boldsymbol{a}_n - \boldsymbol{x}_i)^T (\boldsymbol{a}_n - \bar{\boldsymbol{x}}_i) \tag{18}$$

where $\bar{x}_i$ is the sensor position estimated in the previous iteration. In the light of above, the optimization problem in (15) is expressed as

$$\underset{\boldsymbol{x}_i, t, n}{\text{Min}} \quad \sum_{(n) \in \xi} t_n - \epsilon \sum_{(n) \in \xi} (\boldsymbol{a}_n - \boldsymbol{x}_i)^T (\boldsymbol{a}_n - \bar{\boldsymbol{x}}_i) \tag{19a}$$

$$\text{Subject to} \quad \|\boldsymbol{a}_n - \boldsymbol{x}_i\|_2 \leq r_{ni} + t_n \tag{19b}$$

$$\boldsymbol{x}_i, \boldsymbol{a}_n \geq \mathbf{0} \tag{19c}$$

Here, t_n's are slack variables to be minimized. Moreover, (17) is integrated to the problem by minus sign in the cost function (19a). Hence, the estimated distances in (19b) are minimized and the sum of estimated distance squares in (19a) are maximized. Therefore, $\boldsymbol{x}_i$'s are found such that the estimated distances converge to r_{ni}'s. After all these modifications, the problem in (19a-19c) becomes a modified version of the original problem in bi-convex form. This allows us to find a solution using a convex optimization solver, such as CVX [9].

VI. SIMULATION RESULTS

In this section, the effectiveness of the proposed path planning algorithm (PA) and the localization algorithm (AMA) are justified. PA is compared with the adaptive path planning algorithm in [5] and VB-ERL in [4]. Unless otherwise is stated, the settings given in Table 1 are used for the simulations.

The MA is located at the center of the surveillance region initially and moves $1000s$. The adaptive path planning algorithm in [5] is abbreviated as AA. The number of unknown sensor positions are expressed as residue unknowns.

TABLE I: Parameter settings for the simulations.

L = 100m	$\bar{p}$ = 1m/s	F_{RP}= 3
R = 5m	$\bar{d}$ = 90 Deg.	F_{AT} = 5
α = 0.75	P_{max} = 3m/s	τ = 2
σ = 1	P_{min} = 0.5m/s	ξ = 5
Broadcast Time = 1s	N = 30	λ = 4

In Figure 3, $\mathbf{F}_{RP}$ is swept from 0.1 to 5 for N=30 and the MA movement times are 600s, 800s and 1000s. The average number of residue unknowns for PA are compared with AA in Figure 3. As it is seen, the contribution of virtual attractive force in PA boosts the performance. Less sensors remain unknown in PA compared to AA [5]. For 1000s run, almost all sensors are localized in PA while AA still has 3 residue unknowns. When the remaining unknowns are more than 6 for AA at 1000s, only 1 sensor remains unknown in PA. Hence, when there is control over the velocity and the direction of the MA for sparsely and densely populated areas, more sensors are reached and located for various F_{RP} values.
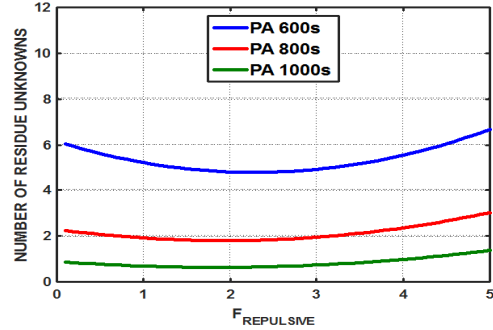
(a) Proposed Algorithm (PA)
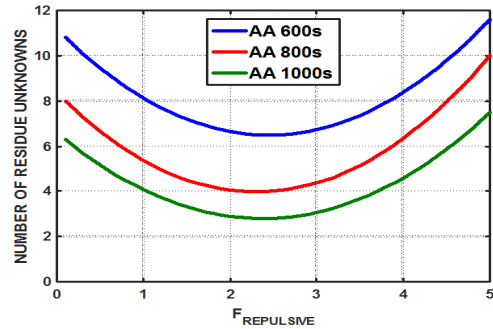
(b) Adaptive Path Planning in [5] (AA)

Fig. 3: Number of unknown sensor nodes remaining vs $\mathbf{F}_{rep}$.

In Figure 4, $P_{max} = 3.5m/s$, P_{min} is swept form 0 to 1m/s by 0.1m/s for N=30 and 50. Other parameters are the same. Figure 4 shows the number of residue unknowns with respect to P_{min}. As P_{min} increases for N=50, the average number of residue unknowns increases from 1.3 to 1.7 in PA while it increases from 5 to 15 for AA. For various sensor numbers, PA localizes more sensors than AA. Besides, the residue unknowns for PA varies more slowly than AA which

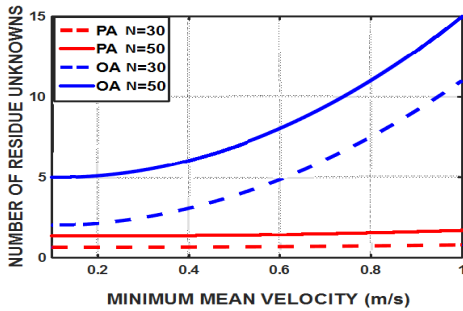shows that AA is more vulnerable to velocity mean changes.

Fig. 4: Residue unknown nodes vs. Pmin

In Figure 5, $P_{max} = 3.5m/s$, $P_{min} = 0$, $\mathbf{F}_{RP} = 3$, the movement time is swept from 1 to 3000 by 10, other parameters remain fixed. Results show that PA covers %80 of the region at 360s. However, AA in [5] and VB-ERL algorithm in [4] reach %80 coverage at 875s and 2150s respectively. Since it is directed to the grids with the least number of anchors, the virtual attractive force provides the MA with more coverage in shorter time than other methods.
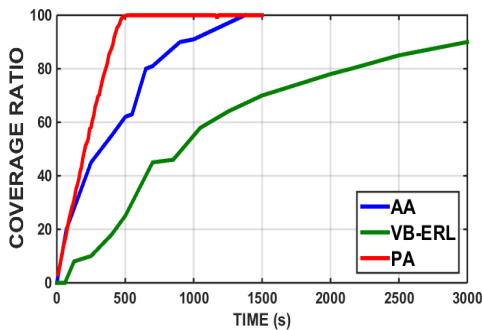

Fig. 5: Coverage ratios of the proposed algorithm, the adaptive algorithm in [5] and VB-ERL in [4]

In Figure 6, linear localization in [6] and localization with AMA are implemented in PA. For $\xi = 5$, movement time=$1000s$ and $P_{max} = 3.5m/s$, the noise variance σ for distance measurements is swept from 0.1 to 2 by 0.1. RMSEs between the real and calculated sensor positions are compared for two methods. As in Figure 6, after σ=0.3, AMA has lower error than the linear localization in [6] for the same number of residue unknowns.
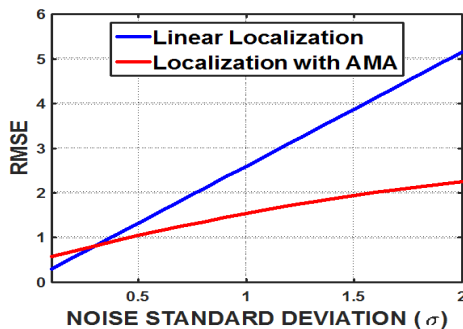

Fig. 6: Efficiency curve of AMA and linear localization

AMA is implemented in PA as the localization method and the performance is expressed in Figure 7. The MA movement time is 1000s and the anchor threshold ξ is swept from 2 to 7 for different noise variances σ. Since AMA lets ξ to be as small as 2, it also increases the performance of path planning algorithm in terms of residue unknowns. As in Figure 7, lower anchor threshold leads to less residue unknowns for the same movement time.
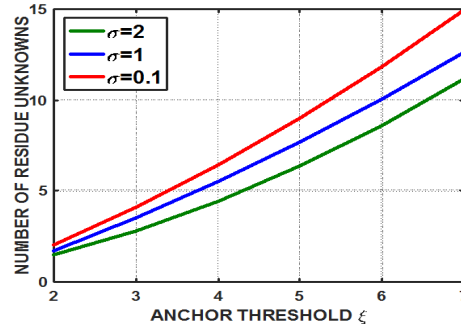

Fig. 7: Residue unknown vs. anchor threshold ξ

VII. CONCLUSION

In this work, a path planning algorithm based on the GM mobility model is proposed for mobile anchor based wireless sensor network localization. Alternating minimization algorithm is used for localizing the sensors. In this approach, by defining a virtual attractive force, a control mechanism is created on the MA direction for sparsely and densely populated areas. Besides, the non-convex structure of the localization problem is converted into a bi-convex form and solved with AMA. The simulation results show that the virtual attractive force strategy increases the number of localized sensors significantly. Moreover, applying AMA provides a faster coverage for path planning, since it requires less anchors for localization. The alternating minimization also increases the localization accuracy compared to the linear localization.

REFERENCES

[1] D. Ciuonzo, P. Salvo Rossi, P. Willett, Generalized Rao Test for Decentralized Detection of an Uncooperative Target. IEEE Signal Processing Letters, 2017.

[2] C. Ou and W. He, Path planning algorithm for mobile anchor-based localization in wireless sensor networks, IEEE Sens. J., vol. 13, no. 2, pp. 466475, Feb. 2013.

[3] N. Patwari, J. Ash, S. Kyperountas, A. Hero, III, R. Moses, and N.S. Correal, "Locating the nodes:Cooperative localization in wireless sensor networks, " IEEE Signal Proc. Mag., vol.22, no.4, pp.5469, Jul. 2005

[4] X. Kuang, H. Shao, and R. Feng, "A new distributed localization scheme for wireless sensor networks, " *Acta Automatica Sinica*, vol. 34, no. 3, pp. 344-348, 2008

[5] Z. Zhong, D. Luo, S. Liu, X. Fan, and Z. Qu, "An adaptive localization approach for wireless sensor networks based on Gauss-Markov mobility model, " *Acta Automatica Sinica*, vol. 36, no. 11, pp. 1557-1568, 2010

[6] F. Liu, H. Zhu, Z. Gu, and Y. Liu, A linear localization algorithm for wireless sensor network based on RSSI, in Advanced Research on Computer Education, Simulation and Modeling, vol. 176, S. Lin and X. Huang, Eds. Berlin, Germany: Springer-Verlag, 2011, pp. 384389.

[7] Liang B, Haas Z J. "Predictive distance-based mobility management for PCS networks," In: Proceedings of the 18th Annual Joint Conference of the IEEE Computer and Communications Societies. New York, USA: IEEE, 1999, pp 1377-1384

[8] I. Csiszr and G. Tusndy, "Information geometry and alternating minimization procedures, " Statistics and Decisions, Suppl. Issue 1, pp.205-237, July 1984.

[9] CVX. [Online]. Available: http://www.cvxr.com